A Tibial Mid-Shaft Injury Mechanism in Frontal Automotive Crashes

Atsutaka Tamura, Katsuya Furusu, Kazuo Miki
Toyota Central R&D Labs., Inc.
Junji Hasegawa
Toyota Motor Corporation
King H. Yang
Bioengineering Center, Wayne State University

Abstract

Lower extremity injuries in frontal automotive crashes usually occur with footwell intrusion where both the knee and foot are constrained. In order to identify factors associated with tibial shaft injury, a series of numerical simulations were conducted using a finite element model of the whole human body. These simulations demonstrated that tibial mid-shaft injuries in frontal crashes could be caused by an abrupt change in velocity and a high rate of footwell intrusion.

1. Introduction

Over the years, a great deal of literature has been devoted to advance our understanding of the biomechanics of lower extremity injuries due to vehicular crashes. However, lower limb injuries are still frequently associated long-term impairments in many crash victims. Many finite element (FE) models of the lower limb have been developed [1, 2, 4, 5] to study injury mechanisms due to difficulties in obtaining test specimens and conducting such experiments. Except for the study reported by Kitagawa et al. [5], which studied pylon fractures of the distal tibia, all other models have focused on the foot and ankle region. On the contrary, tibial shaft fractures frequently occur in the middle portion of the tibia in actual automobile accidents [6, 9, 17, 18], yet such injuries have not been studied extensively. Tamura et al. [15] developed a lower extremity model and validated it against both quasi-static and dynamic test results. Later, Iwamoto et al. [4] used this model to evaluate the efficacy of the tibia index in assessing lower extremity injuries. In this study, a parametric analysis was conducted using the numerical model developed by Tamura et al. in order to extract the most injurious factors that lead to tibial shaft fractures. The selection of these parameters was based on the experimental design method proposed by Taguchi [14]. It was hoped that results from this numerical simulation study would shed some light on the mechanism of tibial shaft fractures.

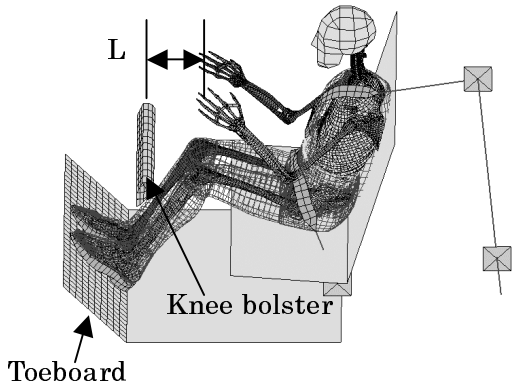

Figure 1. Frontal crash simulation model

2. Methods

2.1 Design of Experiments

Design of experiments (DOE) is a powerful statistical technique introduced in the 1920's to simultaneously study the effects of multiple variables on outcome. The standardized technique of DOE, popularly known as the Taguchi method or the Taguchi approach, was introduced in the U.S.A. in the early 1980's [14]. The main advantage of the

Taguchi method is that, in most cases, the number of experiments required for statistical analyses is less than that of any other statistical method. The concept of integrating Taguchi's DOE and FE methods has been used as design tools in many engineering fields. This integrated approach has the merits of both Taguchi's design of experiments and FE methods. However, previous finite element models developed to study lower extremity injury have not used this technique to check the contribution or significance of each variable that might affect the predictions of the model. In this study, both the Taguchi method and a FE model (Figure 1) were utilized in order to obtain the significance and appropriate level of influence for each of the design variables which were responsible for fractures of the tibial mid-shaft. The occupant model used in this simulation was restrained by a combination of the knee bolster and a 3-point belt system.

Previous studies have identified that knee contact and footwell intrusion in frontal car crashes are often responsible for lower limb injuries [6, 7, 17]. Because the footwell intrusion can be de-coupled into translation and rotation of the toeboard, the three design variables chosen were the distance between the knee and the knee bolster, the rotational angle of toeboard, and the translational intrusion of toeboard. Additionally, the velocity change during the crash was selected as a parameter that would affect the outcome of the model's predictions. Altogether, four 2-level factors were adopted as boundary conditions for the model input as shown in Tables 1 and 2. Table 1 presents an assignment array of four 2-level factors assessed by the Taguchi Method and Table 2 shows a combination of parameters based on this assignment array. Two interactive effects between delta-V and delta-theta, and delta-V and delta-X should have appeared in columns E1 and E2, however, they did not appear in either column. Instead, they were pooled with E3 for error estimation due to the small number of trials. The selection of the parameters listed in Table 2 is justified here. Based on the review of real life accidents [13], the majority of car crashes were found to occur at a delta-V of 55 km/h or less. In the case of an offset car to car crash between vehicles of the same weights, the crash energy of a 55 km/h delta-V is equivalent to a 64 km/h delta-V offset deformable barrier (ODB) crash. In this study, relative velocity changes (delta-V) for level-1 and level-2 design variables were selected as 32 km/h and 64 km/h, respectively. The two-level distance L between the occupant's knee and the knee bolster was set at 65 mm and 130 mm, based on the earlier experiments designed to study the effect of dynamic impact loading on the femur [3]. The toeboard rotation (delta-theta) and the toeboard translation (delta-X) time histories were assumed to have characteristics as shown in Figures 2 and 3, which were obtained from an ODB computer simulation with a delta-V of 64 km/h, while the delta-theta and delta-X time histories for level-2 were assumed to be double that selected for level-1. Furthermore, analyses of the eight frontal crash simulations listed in Table 2 were subdivided into two phases corresponding to the period prior to and that following 60 ms, at which point the knee contacted the knee bolster. In phase 2, the rate of change for both delta-theta and delta-X were much greater than that of phase 1, as shown in Figures 2 and 3.

Table 1. Four 2-level factors assignment array

	ΔV (km/h)	**Δθ (deg)**	E1	**ΔX (mm)**	E2	**L (mm)**	E3
A	1	1	1	1	1	1	1
B	1	1	1	2	2	2	2
C	1	2	2	1	1	2	2
D	1	2	2	2	2	1	1
E	2	1	2	1	2	1	2
F	2	1	2	2	1	2	1
G	2	2	1	1	2	2	1
H	2	2	1	2	1	1	2

Table2. Combination of parameters

	ΔV (km/h)	**Δθ (deg)**	**ΔX (mm)**	**L (mm)**
A	32	17	55	65
B	32	17	110	130
C	32	34	55	130
D	32	34	110	65
E	64	17	55	65
F	64	17	110	130
G	64	34	55	130
H	64	34	110	65

(Maximum values are listed at $\Delta\theta$ and ΔX.)

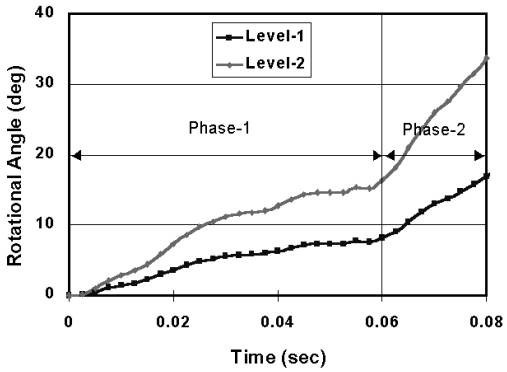

Figure 2. Rotational angle of toeboard at level-1 and level-2

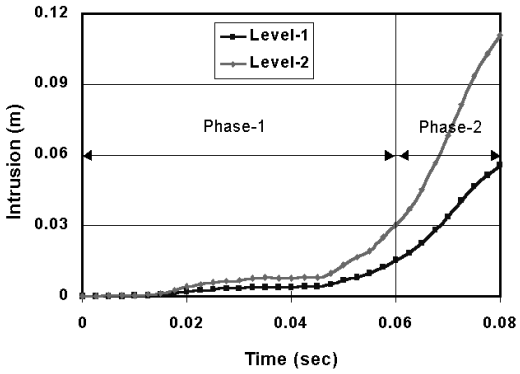

Figure 3. Translational intrusion of toeboard at level-1 and level-2

2.2 Results

Figure 4 shows the axial force and bending moment of the femur for Case F. This figure demonstrates that the changes were more dramatic during phase 2 of the simulation. The maximum axial forces and bending moments of the tibia were determined for each simulation. Simulation results were divided into groups based on four factors (delta-V, delta-theta, delta-X and distance L). Average values for maximum tibial force and maximum tibial moment were calculated. These values are listed in Table 3. Variance analyses were conducted using Excel 2000 (Microsoft Co.) and a low variance ratio of 2.0 was selected as a threshold in order to ensure that important affecting factors would not be missed when calculating significances. As listed in Table 4, rotational angle of the toeboard (delta-theta) and relative velocity change (delta-V) were strongly associated with the increase in the axial force on the tibia. Bending moment of the tibia correlated well with the increase in delta-V and delta-X.

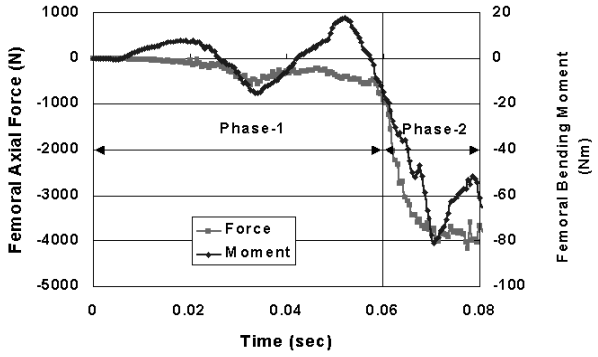

Figure 4. Femoral diaphysis responses obtained from Case F

Table 3. Comparison of the averaged maximum values obtained from tibial shaft responses

	Phase	ΔV	(km/h)	Δθ	(deg)	ΔX	(mm)	L	(mm)
		32	64	17	34	55	110	65	130
Tibial Force	1	938	1010	758	***1190***	924	1020	974	975
(N)	2	1060	1280	1090	1250	1170	1170	1230	1110
Tibial Moment	1	-52.0	***-74.1***	-62.5	-63.6	-58.1	-68.0	-69.3	-56.8
(Nm)	2	-71.6	***-140.7***	-100.6	-111.7	-93.6	-118.8	-100.7	-111.6

Table 4. Results from variance analyses of tibial shaft injury

	Phase	ΔV	Δθ	ΔX	L
Tibial Force	1		○ **		
	2	○	○		
Tibial Moment	1	○ *		○	○
	2	○ **		○	

(*: $p<0.05$, **: $p<0.01$)

3. Discussion

3.1 Assumption for the tibial diaphysis fracture mechanism

Establishing an injury mechanism for fractures of the tibia requires knowledge of peak loads and the sequence of knee and ankle contact. Injury tolerances for the tibia reported in the literature were compared with simulation results. In all cases simulated, the maximum tibial force was less than 1.3 kN (Table 3), which is approximately 16% of the tibial injury criterion of 8.0 kN for impact loading in the axial direction [16, 20]. The low magnitude of axial force predicted by the model indicates that the bending moment in the tibia, rather than the axial force, may be responsible for the occurrence of tibial fracture. Several experimental studies have been conducted to determine the injury tolerance of the tibia when subjected to a 3-point bending. Schreiber et al. [11, 12] reported a tolerance value of 241 Nm based on testing of axially preloaded cadaveric lower leg specimens consisting of the tibia, fibula and surrounding soft tissues tested in 3-point bending with load applied in the posterior-anterior direction. Yamada [8, 19] reported a quasi-static tolerance of 208 Nm, which was obtained utilizing cadaveric specimens from 20 to 39 years of age. In these experiments, tibia only specimens were tested in 3-point bending, loaded along the anterior-posterior direction. Because our intent is to determine the injury mechanism of the tibia, 208 Nm reported by Yamada was adopted as the threshold for tibial shaft fracture. Figure 7 shows the trend observed in the maximum tibial bending moment as a function of delta-V. While other parameters such as delta-X, delta-theta and distance L all need to be considered, it is decided that delta-V needs to be considered first. Based on a simple linear extrapolation, it is expected that a delta-V of 96 km/h is needed in order to reach the threshold of 208 Nm for the tibial bending moment. Sakurai [10] studied the lower extremity response in an experimental study of car to car offset frontal collisions with a relative change in velocity of 100 km/h. He found that the knee contact occurred following the foot to toeboard contact, as evidenced by the peak axial force measured in the tibia. This was observed prior to the occurrence of peak axial load in the femur. Based on the above information, we hypothesize that the tibia must go through the following stages of loading in order to fracture at the mid-shaft:

1. Foot to toeboard contact occurs.
2. Intrusion of the toeboard and forward movement of the occupant act to lock the ankle in dorsiflexion and constrain the distal tibia.
3. Knee to knee bolster contact occurs. The knee bolster and the forward movement of the occupant constrain the proximal tibia.

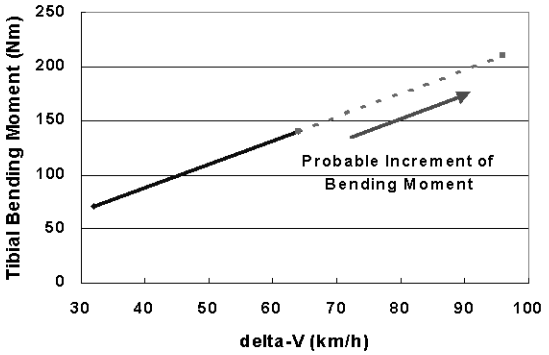

Figure 5. Predicted increase of maximum tibia bending moment

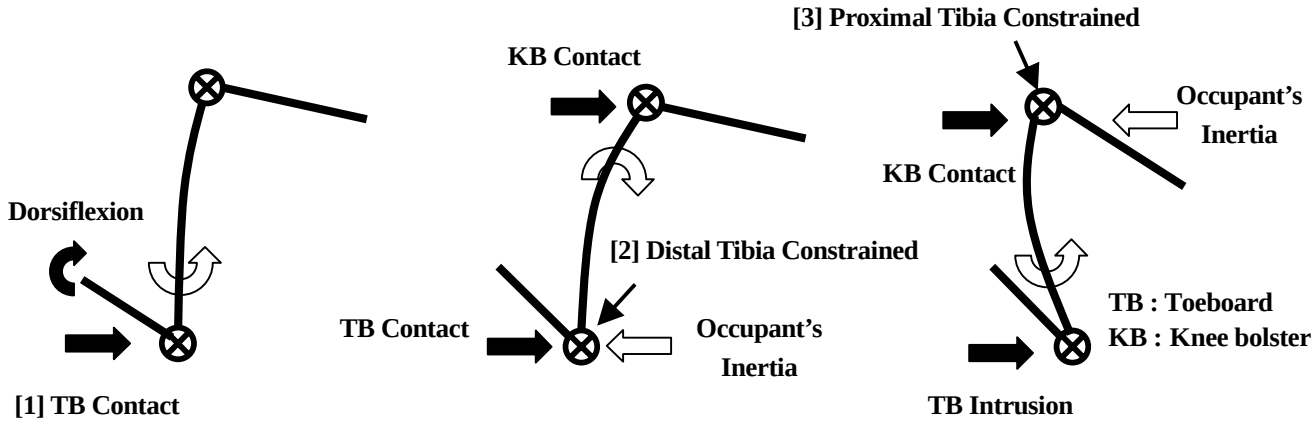

Figure 6. Proposed mechanism of tibial shaft fracture

This hypothetical contact sequence is illustrated in Figure 6. As depicted in this figure, excessive toeboard intrusion at stage 3 will increase the bending moment of the tibia and result in fracture. To study the effect of excessive toeboard intrusion, a maximum value of 340 mm was assumed and computer simulations were repeated. The selection of this distance was based on a study reported by Sugimoto et al. [13] in which car to car offset crashes with a delta-V of 56 km/h were conducted. In these tests, toeboard intrusions ranged from 250 to 300 mm. Because delta-theta was determined to be an insignificant factor by variance analyses, as listed in Tables 3 and 4, the delta-theta was assumed to be 8.5 degrees. Delta-V and L, the distance from the knee to the knee bolster, were assumed to be 96 km/h and 130 mm, respectively. When considering these parameters, the results of the computer simulation demonstrate that the occupant's kinematics follow the three stages of loading described previously. Figures 7, 8 and 9 show the von Mises stress distribution, model-predicted forces and moments, and the kinematics of the occupant at three different times, respectively. As shown in Figure 7, the maximum von Mises stress of the cortical bone exceeded the ultimate strength of 140 MPa, reported by Yamada [19] for the mid-shaft of the tibia. Additionally, the maximum bending moment of the tibia almost reached the critical value of 208 Nm (Figure 8). Results from this simulation support the hypothesis that the likelihood of diaphyseal fracture of the tibia during a frontal car crash increases when the proximal end of the tibia is constrained while the distal end of the tibia is loaded as a result of excessive toeboard intrusion. This loading mechanism due to toeboard intrusion could induce bending of the tibia along its natural bowing curvature and make it vulnerable to fracture. It should be noted that this simulation did not use damageable elements to model the tibia. Thus, tibial shaft fractures cannot be observed visually in the FEM simulation.

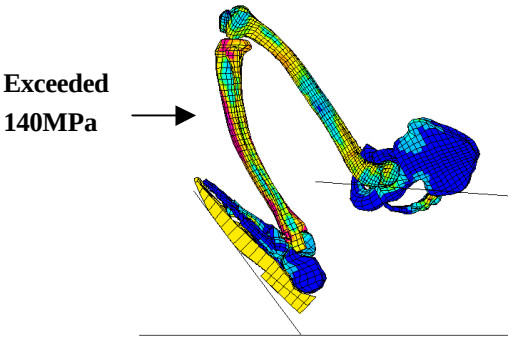

Figure 7. Von Mises stress distribution at T=76 (msec)

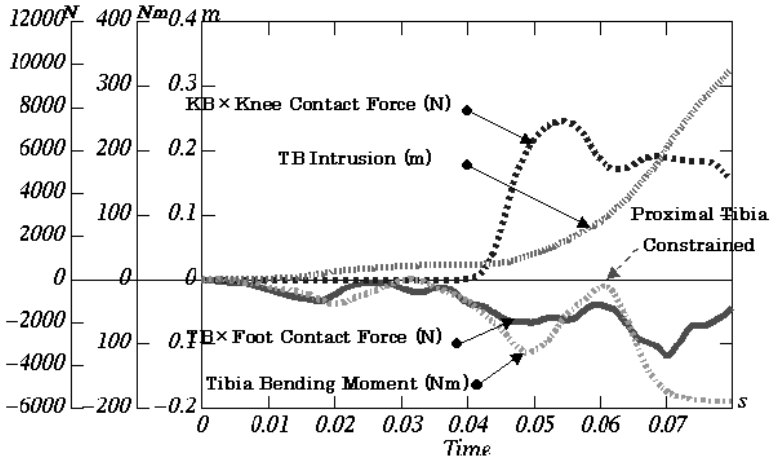

Figure 8. Calculated results in the case of excessive toeboard intrusion

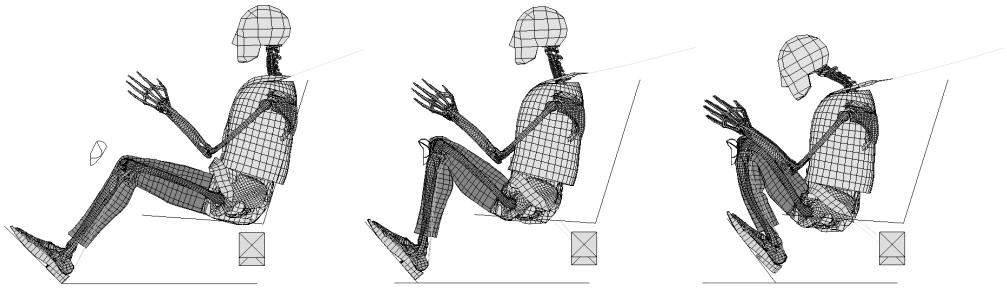

[1] T=0(msec) [2] T=60(msec) [3] T=76(msec)

Figure 9. Occupant's kinematics induced by excessive toeboard intrusion

3.2 Excessive toeboard intrusion under static environment

In order to confirm the hypothesis that inertial effects are essential in producing tibial fractures during frontal crashes, delta-V was reduced to zero while other parameters remained the same. Without the inertial effects, the knee was no longer constrained during the simulation. However, dorsiflexion of the ankle still occurred because the toeboard intrusion was not reduced. Results predicted by the model and occupant kinematics are shown in Figures 10 and 11. As demonstrated by these figures, the maximum bending moment did not exceed 100 Nm throughout the entire simulation.

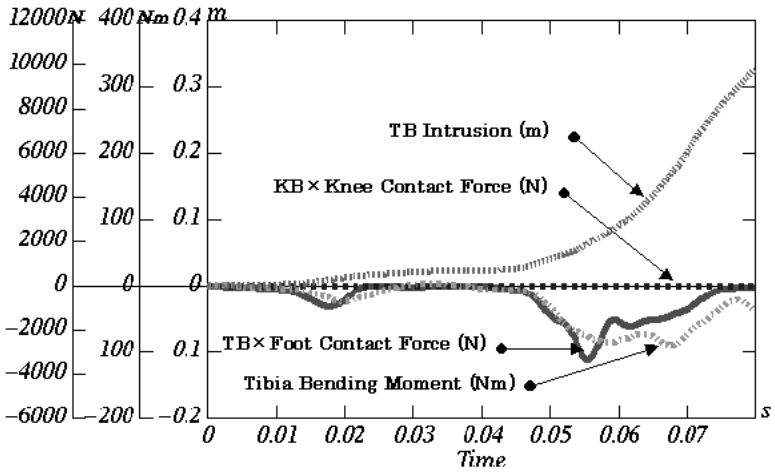

Figure 10. Calculated results obtained from static environmental simulation

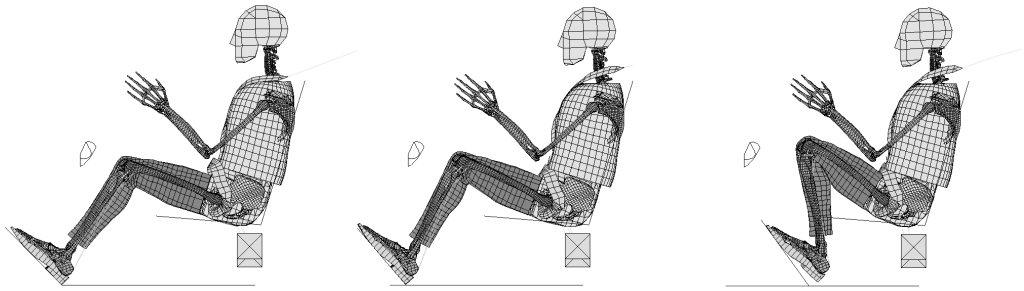

[1] T=0(msec) [2] T=56(msec) [3] T=80(msec)

Figure 11. Occupant's kinematics obtained from static environmental simulation

4. Conclusion

A parametric study of four 2-level factors based on the methods of experimental design proposed by Taguchi has been conducted to determine which factors are most likely to induce tibial shaft fractures. Analysis of variances suggests that abrupt changes in velocity (delta-V) and high rates of toeboard intrusion (delta-X) are the two most profound factors leading to tibial shaft fracture. Computer simulations conducted in the current study enable us to provide useful insight that may be used in the design of safety restraint systems to prevent lower extremity injury without running numerous sled tests. Based on these simulations, a possible mechanism of tibial shaft fracture can be proposed. This mechanism is illustrated in Figure 12 and described in the following statements:

Phase 1 (before 60msec):

[1] Foot to toeboard contact occurs and causes dorsiflexion of the ankle.

Phase 2 (after 60msec):

[2] Excessive dorsiflexion, as well as the inertia of the occupant, lock the position of the distal tibia. Then, knee contact occurs and generates a bending moment in the tibial diaphysis.

[3] Knee bolster, as well as the inertia of the occupant, constrains the proximal tibia. A high rate of toeboard intrusion increases tibial bending moment and causes the

tibia to fracture in the mid-shaft.

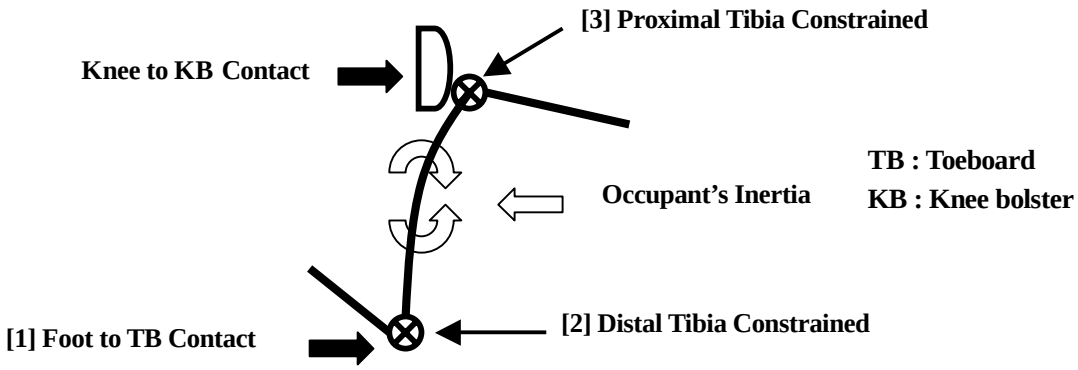

Figure 12. Schematic of tibial shaft fracture mechanism

5. Future work

Material properties used in this lower extremity model are based on stress-strain data obtained from quasi-static tensile tests conducted by Yamada [19]. More detailed investigations are needed to assure that tibial shaft fractures actually do occur at the static bending moment criterion of 208 Nm. Also, strain rate dependency was not considered in the current study and should be taken into account in future studies.

Acknowledgments

The authors would like to thank Ms. Chiharu Kato at Toyota Central R&D Labs., Inc. for her invaluable contribution to this work. We also wish to thank Toyota System Research Inc. for their cooperation.

References

1. Beaugonin M., Haug E., Cesari D., "A Numerical Model of the Human Ankle/Foot under Impact Loading in Inversion and Eversion", Proc. of 40th Stapp Car Crash Conf., #962428, pp. 1-11, 1996.
2. Beaugonin M., Haug E., Cesari D., "Improvement of Numerical Ankle/Foot Model: Modeling of Deformable Bone", Proc. of 41st Stapp Car Crash Conf., #973331, pp. 225-237, 1997.
3. Cheng R., Yang K. H., Levine R. S., King A. I., "Dynamic Impact Loading of the Femur Under the Passive Restrained Condition", SAE #841661, 1984.
4. Iwamoto M., Tamura A., Furusu K., Kato C., Miki K., Hasegawa J., Yang K. H., "Development of a Finite Element Model of the Human Lower Extremity for Analyses of Automotive Crash Injuries", SAE Paper No. 2000-01-0621, SAE 2000 World Congress, 2000.
5. Kitagawa Y., Ichikawa H., King A. I., Levine R. S., A Severe Ankle and Foot Injury in Frontal Crashes and Its Mechanism, Proc. of 42nd Stapp Car Crash Conf., #983145, pp. 1-12, 1998.
6. Morgan R. M., Eppinger R. H., Hennessey B. C., "Ankle Joint Injury Mechanism for Adults in Frontal Automotive Impact", Proc. of 35th Stapp Car Crash Conf., #912902, pp.189-198, 1991.
7. McMaster J., Thomas P., Wallace W. A., Lowne R., "The Mechanism of Below Knee Injury in Frontal Collisions: An Accident analysis study", Proc. of IRCOBI Conf., pp. 483-485, 2000.
8. Nyquist J. W., "Injury Tolerance Characteristics of the Adult Human Lower Extremities Under Static and Dynamic Loading", SAE #861925, 1986.
9. Rommens P., Schmit-Neuerburg K. P., "Ten Years of Experience with the Operative Management of Tibial Shaft Fractures", J. of Trauma, pp. 917-927, 1987.
10. Sakurai M., "Accident Reconstruction Test of Car-to-Car Offset Frontal Collision -Experimental Simulation of Impact Situation Causing the Driver's Ankle Joint Fracture-", Journal of Japan Automobile Research Institute, 19-5, pp. 21-24, 1997.
11. Schreiber P., Crandall J., Micek T., Hurwitz S., Nusholtz G. S., "Static and Dynamic Bending Strength of the Leg", Proc. of IRCOBI Conf., pp. 99-113, 1997.
12. Schreiber P., Crandall J., Hurwitz S., Nusholtz G. S., "Static and Dynamic Bending Strength of the Leg", IJCrash 1998 Vol 3 No 3, pp. 295-308, Woodhead Publishing Ltd, 1998.
13. Sugimoto T., Kadotani Y., Ohmura S., "The Offset Crash Test - A Comparative Analysis of Test Methods", ESV 98-S6-O-08, 1998.
14. Taguchi G., "System of Experimental Design", Kraus International Publications; American Supplier Institute, 1987.
15. Tamura A., Furusu K., Iwamoto M., Kato C., Miki K., Hasegawa J., "Development of a Finite Element Model of the Human Lower Extremity for Assessing Automotive Crash Injury Potential" in Human Biomechanics and Injury Prevention, Kajzer J., Tanaka E., Yamada H. (Eds.), Springer-Verlag, pp. 111-116, 2000.
16. Tannous R.E., Zhang X. A., Bandak F.A., "A Finite Element-Based Study of Pylon Fracture", Biomechanics Research: Experimental and Computational, Proc. of 26th International Workshop, pp. 107-115, 1999.
17. Taylor A., Morris A., Thomas P., Wallace A., "Mechanisms of Lower Extremity Injuries to Front Seat Car Occupants–An in Depth Accident Analysis", Proc. of IRCOBI Conf., pp. 53-72, 1997.
18. Thomas P., Charles J., Fay P., "Lower Limb Injuries – The Effect of Intrusion, Crash Severity and the Pedals on Injury risk and Injury Type in Frontal Collisions", Proc. of 39th Stapp Car Crash Conf., #952728, pp. 265-280, 1995.
19. Yamada H., "The Strength of Biological Materials", Williams & Wilkins Co., 1970.
20. Welbourne E. R., Shewchenko N., "Improved Measures of Foot and Ankle Injury Risk from the Hybrid III Tibia", ESV 98-S7-O-11, pp. 1618-1627, 1998.